Eur Biophys J (1990) 18:57–62

European Biophysics Journal

Residual motion of hemoglobin-bound spin labels and protein dynamics: viscosity dependence of the rotational correlation times

H. J. Steinhoff

Institut für Biophysik, Ruhr-Universität Bochum, Universitätsstrasse 150, D-4630 Bochum, Federal Republic of Germany

Received June 9, 1989/Accepted in revised form November 21, 1989

Abstract. The residual motion of spin labels bound to cysteine $\beta 93$ and to lysines of methemoglobin has been studied by electron paramagnetic resonance spectroscopy. To separate the influences of the solvent and the protein environment of the label fluctuations, the correlation times, τ, were analyzed as a function of temperature for fixed solvent viscosities, η. Results show that over a wide range of viscosity the dependence of τ on η may be empirically described by a power law $\tau \sim \eta^k$. The exponent k depends strongly on the location of the label on the protein surface. If one regards the spin labels as artificial amino acid side chains, characteristic values of correlation times and amplitudes of the rotational motion at the surface can be given. For $\eta = 1$ cP and $T = 297$ K the correlation time of the labels bound to lysines is found to be $\tau = 9 \cdot 10^{-10}$ s and the rotational diffusion is nearly isotropic. The spin label bound to cysteine $\beta 93$ occupies a protein pocket, its rotational motion is therefore restricted. The correlation time of the label motion within a limited motion cone of semi angle $\theta = 30° \pm 3°$ is found to be $\tau = 1.3 \cdot 10^{-9}$ s for $\eta = 1$ cP and $T = 297$ K.

Key words: Protein dynamics – Spin label – Electron paramagnetic resonance – Hemoglobin – Viscosity

Introduction

Proteins are dynamic systems. In a given conformation, for example the R- or T-structures of hemoglobin, in which the protein performs a particular function, it can assume a very large number of structurally different conformational substates (Gurd and Rothgeb 1979; Frauenfelder et al. 1979). Each individual protein molecule rapidly fluctuates from one substate to another at physiological temperatures. The nature of these motions range from local vibrations of atoms and groups to global changes of relative positions of whole domains, and their characteristic time scales stretch from fractions of picoseconds to seconds. Either type of motion depends in some way on environmental factors such as solvent composition, pH, ionic strength, and viscosity.

The aim of the present paper is to extract information about the dependence of the dynamics of parts of the protein surface on the environmental viscosity, η, using the spin label technique. The influence of Brownian motion of solvent molecules on mobility and reaction rates in proteins is of considerable interest. It has been suggested that solvent-induced structural fluctuations trigger catalysis in enzymes (Careri et al. 1979). Measured rates of various intramolecular activated processes in macromolecules exhibit a dependence on the solvent viscosity which often deviates from the η^{-1}-law derived for one-dimensional models in the limit of high viscosity (Kramers 1940). For conformational transitions of polymers in solution rates $r \sim \eta^{-k}$ with exponents $k = 1$ were found (Bullock et al. 1974). In flash photolysis experiments on myoglobin (Beece et al. 1980) and bacteriorhodopsin (Beece et al. 1981) the viscosity dependence of several successive reaction steps was studied. The authors found exponents k between 0.1 and 0.8 for viscosities $\eta \leq 10^4$ cP. The viscosity dependence of the rates has been attributed to fluctuations between conformational substates. Theoretical models have been shown to predict values of $k \leq 1$ for activated processes in proteins (Doster 1983; Schlitter 1988).

In the present work the rotational correlation times, τ, of nitroxide spin labels covalently bound to hemoglobin have been investigated as a function of solvent viscosity. A protein bound spin label may be regarded as an artificial amino acid side chain. The electron paramagnetic resonance (EPR) spectrum of this label is sensitive to the rate of the nitroxide rotational motion. So the EPR spectrum of a bound label will directly reflect the motion of the macromolecule itself or the fluctuation of macromolecule domains, or some residual motion of the label with respect to the whole macromolecule. It has been shown in an earlier paper (Steinhoff et al. 1989), that the examination of the residual motions of these spin labels gives information about the dynamics of parts of the protein surface. Strong correlation between the proper-

ties of the hydration shell and the label fluctuations has been observed.

The EPR-spectra of the label 4-maleimido-2,2,6,6-tetra-methylpiperidinyl-1-oxyl (Mal6) bound to cysteine $\beta 93$ of methemoglobin are analyzed as a function of temperature and viscosity in different solvent environments. The label occupies the tyrosine pocket of the hemoglobin molecule providing a label position inside the protein close to its surface (Moffat 1971). Additionally the spectra of the label N-(1-oxyl-2,2,6,6-tetramethyl-4-piperidinyl) iodoacetamide (JAA6) bound to lysines at the surface of the protein are examined. Owing to different distances of the NO groups from the protein surface the two systems differ in their possible interaction with the protein and solvent. Angles of the limited motion cone and rotational correlation times of the residual label motion are calculated from the experimental spectra using computer simulations. In interpreting the data we treat the temperature dependence and the viscosity dependence of the observed motions separately and ask about the influence of the solvent on the dynamic properties.

Experimental

Materials and equipment

Oxyhemoglobin was prepared from fresh horse blood samples by the methods of Benesch et al. (1972). Spin labeling (Mal6) of cysteine $\beta 93$ of oxyhemoglobin followed the procedure of McCalley et al. (1972). Lysines of oxyhemoglobin were labeled by incubation with JAA6 spin label at pH 10 for 5 h in borate buffer at 298 K (Karim and Steinhoff, in preparation). The cysteine $\beta 93$ has been previously blocked by iodoacetamide.

The oxidation of the labeled oxyhemoglobin (abbreviated hbcys-Mal6 and hblys-JAA6) to methemoglobin was achieved by addition of a threefold excess of $K_3(Fe(CN)_6)$. The samples were desalted by running through a column of Sephadex G-25. Polycrystalline samples and single crystals were prepared by mixing the solutions of labeled methb with buffered ammonium sulfate solutions according to the method of Perutz (1968).

Mixtures of water with glycerol and sucrose were used to vary the solvent viscosity. Phosphate buffer (50 mM), pH 7 in water, was used for the samples. Solution viscosities were taken from Landolt-Börnstein (1950).

EPR spectra were measured on a home made X-band spectrometer equipped with a modified Oxford ESR 9 variable temperature accessory. The microwave power used was 0.1 mW, the modulation frequency was 52 kHz and the modulation amplitude $0.4 \cdot 10^{-4}$ T. The magnetic field was measured with a Bruker B-NM 12 instrument. 2,2-diphenyl-1-picrylhydrazyl (DPPH) powder served as a g-value standard ($g = 2.0037$). After analog-digital conversion the spectra were recorded by a personal computer (CBM 8296, Commodore) and then transmitted to a Cyber 855 (Control Data).

Theory

Analysis of EPR spectra

EPR spectra were analysed using methods described (Steinhoff et al. 1989; Steinhoff 1988). The degree of averaging of the spectra is characterized by an order parameter S_z defined as

$$S_z = \frac{A'_{zz} - 1/3 \text{ Tr } \mathbf{A}'}{A_{zz} - 1/3 \text{ Tr } \mathbf{A}} \tag{1}$$

A_{zz} is the principle z-value of the electron nuclear hyperfine interaction tensor $\mathbf{A}$, Tr $\mathbf{A}$ is the trace of the tensor. The tensor parameters without primes are the rigid limit values, the primed values are spatial averaged effective tensor values. These values are calculated from experimental EPR spectra by means of least-squares fitting of simulated spectra with a time-independent Hamiltonian

$$H = \beta_e \boldsymbol{S} \mathbf{g} \boldsymbol{H} + \boldsymbol{S} \mathbf{A} \boldsymbol{I} \tag{2}$$

where $\boldsymbol{H}$ is the external field vector, β_e the Bohr magneton, $\boldsymbol{S}$ the electron spin operator, $\boldsymbol{I}$ the nuclear spin operatore, and $\mathbf{g}$ the electron g-value tensor. Parameters of the fitting procedure are the six principal values of the tensors $\mathbf{g}$ and $\mathbf{A}$. Introducing molecular motion with correlation times less than 10^{-7} s the spectrum can be simulated by replacing the tensors $\mathbf{g}$ and $\mathbf{A}$ by spatial averaged effective tensors $\mathbf{g}'$ and $\mathbf{A}'$. This yields a time-independent effective Hamiltonian, H_{eff}. Calibration curves of S_z for the case of isotropic motion in the rotational correlation time range between $6 \cdot 10^{-7} \text{ s} > \tau > 10^{-10}$ s have been calculated by least-squares fitting of generated powder spectra using H_{eff} to spectra calculated using the stochastic Liouville method of Freed (1976). For the case of anisotropic fluctuations of the label molecular z-axis within a limited motion cone of semi angle θ, S_z values have been calculated using EPR spectra simulations on the basis of a two-jump model. The theory of EPR spectra simulation on the basis of this model is given in Steinhoff et al. (1989). Calibration curves of S_z for some selected values of the semi angle θ are given in Fig. 1. So we know how S_z is affected by the rotational diffusion model and the rotational correlation time τ, and it is possible to estimate τ without the necessity of making detailed line-shape calculations if we know θ. The calibration curves of S_z vs. τ can be fitted to the empirical expression

$$\tau = a \left\{ \frac{S_z - S_z(0)}{1 - S_z} \right\}^b \text{ ns} \tag{3}$$

in the range $10^{-9} \text{ s} \leq \tau \leq 10^{-7}$ s to within less than 20% in the value of τ for the isotropic (Brownian diffusion) or two-jump model, with the values of a and b given in Table 1. $S_z(0)$ is the boundary value of S_z for $\tau \to 0$. In the case of isotropic Brownian diffusion $S_z(0)$ equals zero, whereas it depends on the semi angle θ of the limited motion cone in the case of anisotropic fluctuations of the label. The behavior of $S_z(0)$ is given in Fig. 2 for the two-jump model and for a wobbling model with a ran-

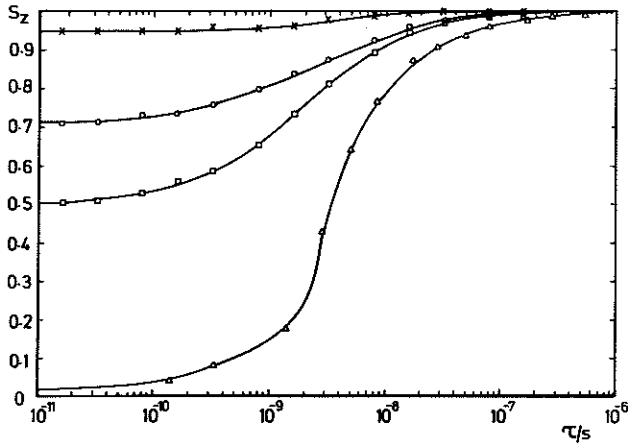

Fig. 1. The parameter S_z versus correlation time for the two-jump model: (×), semi angle $\theta = 12.5°$; (○), $\theta = 30°$; (□), $\theta = 45°$; and for (△) isotropic Brownian diffusion. The curves were determined from fitting of spectra on the basis of the time-independent effective Hamiltonian to spectral simulations using the two-jump model as described in Steinhoff et al. (1989) and the Brownian diffusion model according to the method of Freed (1976)

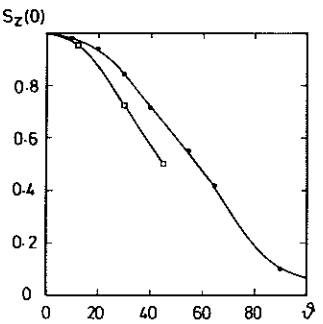

Fig. 2. The boundary value of the parameter S_z, $S_z(0)$, versus the semi angle of the limited motion cone θ for two rotational diffusion models: (□), two-jump model; (○), wobbling model with a random distribution of the label molecular z-axis (calculations by K. Lieutenant)

Table 1. Parameters for fitting (3), peak-peak line width $\delta = 3$ G

Diffusion model	a	b
Brownian diffusion ($S_z(0) = 0$)	3.33	0.91
two-jump model ($S_z(0) > 0.5$)	2.27	0.87

dom distribution of the label molecular z-axis in a limited motion cone of semi angle θ (Lieutenant, unpublished results). Thus we note that a change in S_z can arise from a real change in the angle θ or a change in the rotational rate. In general these two phenomena cannot be distinguished unless the rotational correlation time falls into a time range where S_z reaches the limit $S_z(0)$, that means $\tau < 10^{-10}$ s. The determination of $S_z(0)$ – and therefore θ – from the experimental data is described in the next section. All calculations and spectra simulations were executed on a CYBER 855 computer.

Results and discussion

Determination of τ and $S_z(0)$

The behavior of the parameter S_z with temperature for polycrystalline methbcys-Mal6 and samples of methbcys-Mal6 in solutions of different viscosity is shown in Fig. 3. The values of S_z of all samples decrease with increasing temperature. It has been shown in Steinhoff et al. (1989) that the variation of S_z for the polycrystalline sample can quantitatively be explained by two motional mechanisms. A fast vibration of the label ($\tau < 10^{-12}$ s) with an angular amplitude (in radians) of wobbling oscillation of the label molecular z-axis of

$$\phi = \sqrt{R\,T/E_a} \tag{4}$$

which yields

$$S_z = 3/4 \sin\phi \cos\phi/\phi + 1/4$$

is responsible for the observable decrease in S_z up to temperatures of 200 K (cf. Fig. 3a). The potential energy barrier E_a characterizing this vibration is determined by a fitting procedure (Johnson 1981). Measurements of the dependence of E_a on the degree of hydration have shown that E_a increases with increasing water content of the sample (Steinhoff et al. 1989). Additionally a second kind of motion becomes visible above 200 K for water containing samples (cf. Fig. 3b). The temperature dependence of this motional process can quantitatively be accounted for by an activated process, where the correlation time τ of (3) is parameterized with the Eyring relation:

$$\tau = \nu^{-1} \exp(\Delta G^*/R\,T)$$
$$\Delta G^* = \Delta H^* - T\,\Delta S^* \tag{5}$$

$R = 8.31$ J mol^{-1} and we take the frequency factor ν to be temperature independent, $\nu = 10^{+13}$ s^{-1}. ΔG^* is the activation Gibbs energy, with the activation enthalpy ΔH^* and entropy ΔS^*. Examples of the fits of (3) and (5) to the experimental data are shown in Fig. 3b. Values of the fit parameters ΔH^*, ΔS^* and $S_z(0)$, which are assumed to be temperature-independent in the temperature range examined, are given in Table 2. In these fit procedures the additional influence of the vibration process on S_z has been considered, the values of E_a had been determined by an independent fit with a high temperature cut off at $T = 190$ K. Though the activation entropy and enthalpy depend on the system under consideration (cf. Table 2), the boundary values $S_z(0)$ coincide within experimental error. The angle θ of the limited motion cone for the three systems, polycrystalline methbcys-Mal6, methbcys-Mal6 in glycerol-water and in sucrose-water solution, are found to be $30° \pm 3°$ on the basis of the two-jump model (cf. Fig. 2).

The assumption of a temperature-independent value of the angle θ is justified by an observation on methbcys-Mal6 single crystals (Chien 1979). The EPR single crystal line width of methbFcys-Mal6 increases from about 3.5 Gauss at $T = 298$ K to between 15 to 18 Gauss at $T = 77$ K. The change has been ascribed to motional narrowing at room temperature due to a "wiggling" of the

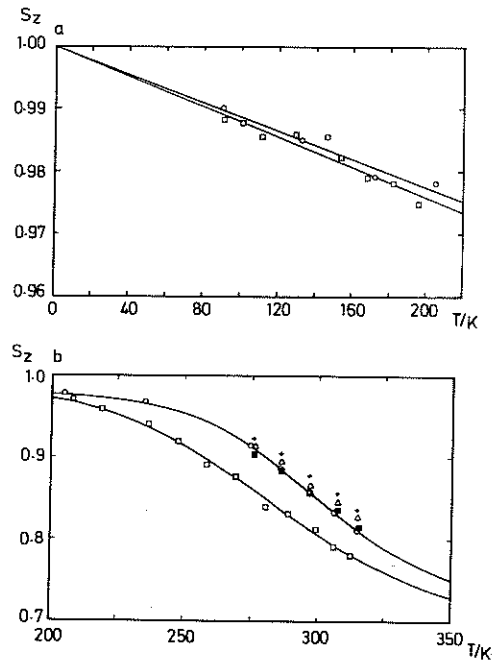

Fig. 3 a, b. Parameter S_z of methbcys-Mal6 samples as a function of temperature. (□), polycrystalline methbcys-Mal6; (○), 87% glycerol-water solution; (■), 65% sucrose-water solution; (△), 70% sucrose-water solution, and (+), 74% sucrose-water solution. **a** Temperature range $T<200$ K. The lines are fits of (1) and (4) (oscillation model) to the experimental data points with parameters E_a and A_{zz}: crystalline sample, $A_{zz}=105.7\pm0.1$ MHz, $E_a=34\pm5$ kJ/mol; glycerol-water solution, $A_{zz}=103.4\pm0.2$ MHz, $E_a=37\pm5$ kJ/mol. **b** Temperature range $T>200$ K. The lines are fits of (3) and (5) to the experimental data points of the polycrystalline sample and the glycerol-water solution. Only five series of measurements and two fits are shown for clarity. The parameters ΔH^*, ΔS^* and $S_z(0)$ of the fits to the complete set of experimental data points are given in Table 2

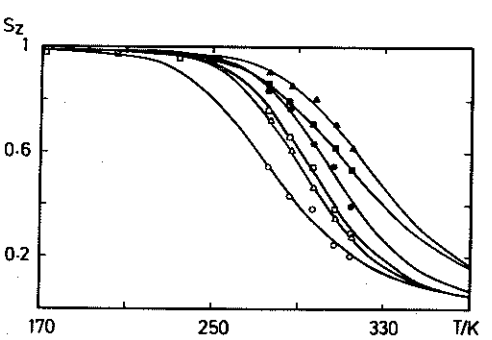

Fig. 4. Parameter S_z of methblys-JAA6 samples in solutions of different viscosities as a function of temperature: (□), 79% glycerol-water solution; sucrose-water solutions of different sucrose concentrations: (○), 50%; (△), 60%; (●), 65%; (■), 67.5%; (▲), 72%. The lines are fits of (3) and (5) to the experimental data points

spin label. The label may be frozen in different orientations relative to the protein molecule at 77 K, leading to the observed broad single crystal lines at this temperature. The line shapes of the first derivative of an EPR powder spectrum at the positions $H\pm=(h\nu\pm A_{zz})/(g_{zz}\beta_e)$ are a good approximation for the line shape of an absorption line of a single label orientation (Weil and Hecht 1963). From experimental powder spectrum of

Table 2. Activation enthalpies and entropies and $S_z(0)$ for the label motion in methbcys-Mal6 ($\nu=10^{13}$ s^{-1})

System	ΔH^*/kJ mol^{-1}	ΔS^*/J mol^{-1} K^{-1}	$S_z(0)$
methbcys-Mal6, polycrystalline	18 ± 2	-23 ± 4	0.70 ± 0.04
in sucrose water solution, 65%	20 ± 3	-19 ± 8	0.70 ± 0.08
67.5%	21 ± 3	-16 ± 12	0.69 ± 0.08
70%	24 ± 5	-7 ± 20	0.73 ± 0.10
72%	21 ± 3	-21 ± 14	0.61 ± 0.18
74%	26 ± 3	-2 ± 12	0.74 ± 0.06
in 87% glycerol-water solution	26 ± 2	3 ± 8	0.73 ± 0.03

methbcys-Mal6 at 77 K we got a line width Δ of a single orientation of 3 Gauss. Using this value of Δ, we simulated single crystal spectra with a random distribution of the label molecular z-axis within a cone of semi angle θ. We get a maximum line broadening of 18 Gauss if we assume a value of θ of 24°. That means that the increase of θ is less than 6° if we increase the temperature from 77 K to 320 K. So the errors in τ will be negligible if we assume $S_z(0)$ to be temperature-independent in the temperature range from 250 K to 320 K. Thus the value of $S_z(0)$ is known (we take $S_z(0)=0.72$ for all methbcys-Mal6 samples), the values of τ for every sample and temperature may be calculated using (3) with the experimental values of S_z. To avoid systematic errors in the determination of S_z and τ due to the rotational diffusion of the whole protein molecule, only data for viscosities $\eta>30$ cP are considered for methbcys-Mal6 samples. In this case the remaining error in τ is less than 5%.

The values of S_z for the methblys-JAA6 samples are shown in Fig. 4 for different temperatures and viscosities. The values of this parameter reflect a greater flexibility of this complex compared to the methb-Mal6 samples. The data points of all samples are well fitted by (3) and (5) assuming a boundary value $S_z(0)=0$. The semi angle θ of the limited motion cone of the molecular z-axis is therefore greater than 90° (cf. Fig. 2). Thus the fluctuations of the labels in these samples are more isotropic than the motion in the methbcys-Mal6 samples and we therefore use the parameters a and b in (3) for isotropic Brownian motion to calculate τ from the experimental data.

The viscosity dependence of τ

In the preceding part we considered the protein and the solvent as one system, and the activation parameters depend on the solvent. In the following part we conceptually isolate the protein and investigate how the solvent influences its properties as suggested in Beece et al. (1980). We use solvents in which we can vary the viscosity η over a wide range keeping the variations of the other variables small. Changing the sucrose concentration from 60% ($T=320$ K) to 74% ($T=273$ K) alters the viscosity by about three orders of magnitude. Moreover, 65% sucrose-water and 87% glycerol-water or 60% sucrose

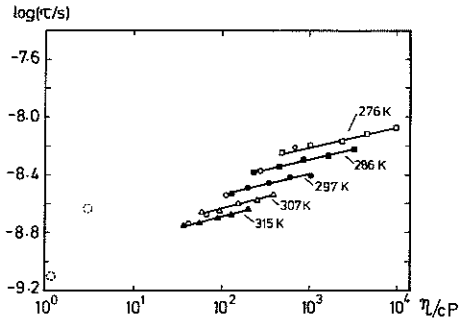

Fig. 5. Isothermal plots of the logarithm of the correlation time, $\log \tau$, versus the logarithm of the viscosity, $\log \eta$, for methbcys-Mal6 samples in sucrose-water solutions: (□), 276 K; (■), 286 K; (●), 297 K; (△), 307 K; (▲), 315 K. The dashed circles are the values for polycrystalline methbcys-Mal6 for 276 K and 315 K. Open circles represent the data points for methbcys-Mal6 in 87% glycerol-water solution

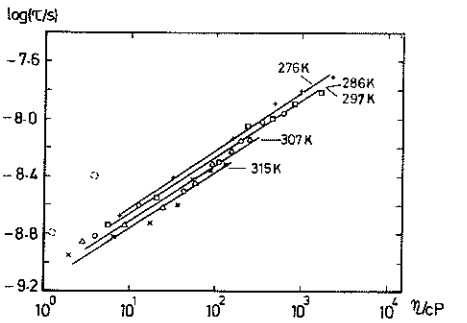

Fig. 6. Isothermal plots of $\log \tau$ vs. $\log \eta$ for methblys-JAA6 samples: (+), 276 K; (□), 286 K; (○), 297 K; (△), 307 K; (×), 315 K. The dashed circles are the values for polycrystalline methblys-JAA6 for 276 K and 315 K

water and 79% glycerol-water, which have the same viscosities at a given temperature, show nearly the same averaging parameter S_z and therefore nearly the same correlation times (cf. Fig. 3b and 4). We consequently assume that the correlation times depend on variables other than T mainly through their dependence on viscosity:

$$\tau = \nu^{-1} \exp\{\Delta G^*(\eta, T)/R\,T\}$$
$$\Delta G^*(\eta, T) = \Delta H^*(\eta) - T\,\Delta S^*(\eta) \qquad (6)$$

To determine ΔH^* and ΔS^* we draw first isothermal plots of $\log \tau$ versus $\log \eta$. These plots are shown in Fig. 5 for the methbcys-Mal6 samples and in Fig. 6 for the methblys-JAA6 samples. Over a wide range in η, $\log \tau$ is approximately proportional to $\log \eta$; τ consequently is proportional to a power of η, $\tau \sim \eta^k$. The exponent k does not significantly depend on temperature in the temperature range investigated. We find $k = 0.2$ and $k = 0.4$ for the two systems respectively. (A plot of $\log \tau$ versus $\log \eta$ for unbound spin label tumbling freely in sucrose-water solution yields $k = 1.0$). These experimentally observed results do not necessarily affect the validity of the standard Stokes-Einstein formula, $\tau = c\,a^3\,\eta/k\,T$. It has been shown by Zwanzig and Harrison (1985) that the exponential behavior of τ with η may be explained by variations of a, which has been characterized as an effective hydrodynamic radius. This effective hydrodynamic radius is regarded as a measure of the strength of short-ranged solute-solvent interaction. In the present case these interactions are very complex as the labels may interact with the protein surface, adjacent amino acid side chains, bound water and the solvent. The solvent viscosity therefore affects fluctuations in a different way, depending on the degree to which motions at the protein surface are involved. The effect of the solvent viscosity is attenuated and shielded, if the motion mainly takes place in the interior of the protein; the coefficient k characterizes this shielding (Beece et al. 1980).

The shielding is obviously more effective in the methbcys-Mal6 samples compared to the methblys-JAA6 system. This can be understood as the label in the methbcys-Mal6 sample is buried inside a pocket at the protein surface (Moffat 1971). The labels bound to lysines in the methblys-JAA6 samples extend into the solvent as we may conclude from the nearly isotropic rotational behavior.

As a consequence the correlation times of the JAA6 label bound to lysines are less than those for the label in the tyrosine pocket for low viscosities ($\eta < 10$ cP) as we can see, if we extrapolate the lines in Fig. 5 to low viscosities. For $\eta = 1$ cP and $T = 297$ K we get $\tau = 0.9$ ns for methblys-JAA6 and $\tau = 1.3$ ns for methbcys-Mal6. For greater viscosities ($\eta > 100$ cP) however, the label fluctuations inside the tyrosine pocket are faster than the motions of the label bound to the lysines. For example, we have $\tau = 2.2 \cdot 10^{-9}$ s for methbcys-Mal6 and $\tau = 5 \cdot 10^{-9}$ s for methblys-JAA6 at $\eta = 200$ cP and $T = 315$ K.

Correlation times of the label fluctuations extracted from polycrystalline samples are also shown in Figs. 5 and 6. We do not know the values of the viscosity of the so called bulk water in methemoglobin crystals. Owing to the crystallization method this bulk water consists of a solution of buffered ammonium sulfate. The viscosity values of a $(NH_4)_2SO_4$ solution of adequate concentration are chosen as a lower limit for η. If we now extrapolate the isothermal lines given for the sucrose-water solutions to lower viscosities we recognize that the experimental results for the crystallized methbcys-Mal6 samples fit these curves well. So the dynamics of the label at the protein surface are not altered by crystallization in this case. In contrast to this observation the correlation times of the label in the crystalline methblys-JAA6 sample are greater than expected from the solution experiments (cf. Fig. 6). This discrepancy may be due to strong interactions of the long lysine-JAA6 side chain with neighbouring hemoglobin molecules in the crystal.

Lines of constant η intersect particular isothermal trajectories; values of $\log \tau$ read from these intersections may be plotted versus $1/T$ for different viscosities. Since k does not depend on temperature or viscosity in the ranges under investigation an Arrhenius plot for only one value of η ($\eta = \text{const} = 300$ cP) is shown in Fig. 7. Correlation times for unbound spin labels (JAA6) tumbling freely in solution are calculated using the Stokes-Einstein formula. This curve is given additionally for comparison. Thus the

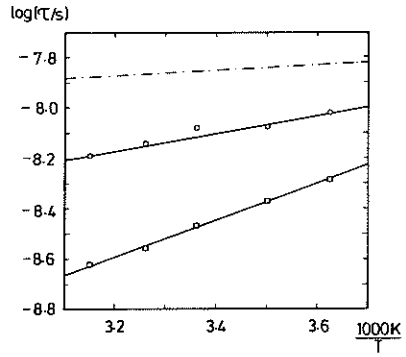

Fig. 7. Isoviscosity Arrhenius plots of the residual motion of hemoglobin-bound spin labels, $\eta = \text{const.} = 300$ cP. (○), methblys-JAA6; (□), methbcys-Mal6. Calculated correlation times for isotropic Brownian diffusion of free spin labels (JAA6) are given for comparison (– · –)

influence of the solvent on the temperature dependence of the motion is eliminated and the remaining temperature dependence of τ is due to the interaction of the label with its environment consisting of parts of the protein and bound water. Enthalpies of activation calculated from the slopes are 14 kJ/mol and 7 kJ/mol for the methbcys-Mal6 sample and the methblys-JAA6 sample respectively. These values are viscosity-independent in the viscosity range from 30 to 10^3 cP. The values of ΔH^* for the two samples indicate that the energy barrier properties of the label motion depend on the specific location of the labels. Movements of adjacent amino acid side chains may be involved in these label fluctuations to a different degree.

In the present paper correlation times and amplitudes for the rotational motion of hemoglobin-bound spin labels are given and their dependence on solvent viscosity is examined. The spin labels may be regarded as artificial amino acid side chains of the protein. Natural amino acid side chains of similar structure and environment should have similar dynamic properties. So the presented data should be characteristic for the dynamics of parts of the protein surface. The interaction between protein and solvent seems to be very complex as we see from the viscosity dependence of the label motion and steric effects may play a large role. Chemical reactions of proteins, for example ligand binding or enzyme catalysis, may be profoundly affected by this interaction and the steric effects remain to be investigated.

Acknowledgements. I should like to thank C. Karim for the preparation of the samples, K. Lieutenant for computer simulations, and A. Redhardt for helpful discussions.

References

Beece D, Eisenstein L, Frauenfelder H, Good D, Marden MC, Reinisch L, Reynolds AH, Sorensen LB (1980) Solvent viscosity and protein dynamics. Biochemistry 19:5147–5157

Beece D, Bowne SF, Czege J, Eisenstein L, Frauenfelder H, Good D, Marden MC, Marque J, Ormos P, Reinisch L, Yue KT (1981) The effect of viscosity on the photocycle of bacteriorhodopsin. Photochem Photobiol 33:517–522

Benesch RE, Benesch R, Renthal RD, Maeda N (1972) Affinity labeling of the polyphosphate binding site of hemoglobin. Biochemistry 11:3576–3582

Bullock AT, Cameron GG, Smith PM (1974) Electron spin resonance studies of spin-labelled polymers. J Chem Soc Faraday Trans II 70:1202–1210

Careri G, Fasella P, Gratton E (1979) Enzyme Dynamics: The statistical physics approach. Ann Rev Biophys Bioeng 8:69–97

Chien JCW (1979) Electron paramagnetic resonance crystallography of spin-labeled hemoglobin-protein fine structure. J Mol Biol 133:385–398

Doster W (1983) Viscosity scaling and protein dynamics. Biophys Chem 17:97–103

Frauenfelder H, Petsko GA, Tsernoglou D (1979) Temperature dependent X-ray diffraction as probe of protein structural dynamics. Nature 280:558–563

Freed JH (1976) Theory of slow tumbling ESR spectra for nitroxides. In: Berliner LJ (ed) Spin labeling theory and applications. Academic Press, New York, pp 53–132

Gurd FRN, Rothgeb TM (1979) Motions in proteins. Adv Protein Chem 33:73–165

Johnson ME (1981) Apparent hydrogen bonding by strongly immobilized spin-labels. Biochemistry 20:3319–3328

Kramers HA (1940) Brownian motion in a field of force and the diffusion model of chemical reactions. Physica 7:284–304

Landolt-Börnstein (1950) Springer, Berlin Heidelberg New York

McCalley RC, Shimshick EJ, McConnell HM (1972) The effect of slow rotational motion on paramagnetic resonance spectra. Chem Phys Lett 13:115–119

Moffat JK (1971) Spin-labelled haemoglobins: A structural interpretation of electron paramagnetic resonance spectra based on X-ray analysis. J Mol Biol 55:135–146

Perutz MF (1968) Preparation of haemoglobin crystals. J Cryst Growth 2:54–56

Schlitter J (1988) Viscosity dependence of intramolecular activated processes. Chem Phys 120:187–197

Steinhoff HJ (1988) A simple method for determination of rotational correlation times and separation of rotational and polarity effects from EPR spectra of spin-labeled biomolecules in a wide correlation time range. J Biochem Biophys Meth 17:237–248

Steinhoff HJ, Lieutenant K, Schlitter J (1989) Residual Motion of hemoglobin-bound spin labels as a probe for protein dynamics. Z Naturforsch 44c:280–288

Weil JA, Hecht HG (1963) On the powder line shape of EPR spectra. J Chem Phys 38:281–282

Wien RW, Morrisett JD, McConnell HM (1972) Spin-label-induced nuclear relaxation. Distances between bound saccharides, Histidine-15, and Tryptophan-123 on lysozyme in solution. Biochemistry 11:3707–3716

Zwanzig R, Harrison AK (1985) Modifications of the Stokes-Einstein formula. J Chem Phys 83:5861–5862